

Gapless state produced in $\text{Hg}_{1-x}\text{Cd}_x\text{Te}$ alloys under pressure

N. B. Brandt, O. N. Belousova, L. A. Bovina, V. I. Stafeyev, and Ya. G. Ponomarev

Moscow State University

(Submitted July 13, 1973)

Zh. Eksp. Teor. Fiz. 66, 330-347 (January 1974)

Transitions to a gapless state (GS), which occur in p -type $\text{Hg}_{1-x}\text{Cd}_x\text{Te}$ alloys as a result of the inversion of the terms Γ_6 and Γ_8 under pressure, are investigated. The galvanomagnetic effects in a weak magnetic field ($2 \leq T < 300^\circ\text{K}$) and the Shubnikov-de Haas effect ($2 \leq T \leq 4.2^\circ\text{K}$) are investigated in a wide pressure interval, $1 \text{ atm} \leq p < 10 \text{ katm}$. It is shown that the specific feature of the transition to the GS in the investigated alloys is due to overlap of the impurity hole band with the conduction band, an overlap amounting to $\sim 3\text{meV}$. A linear decrease of the cross section of the electronic Fermi sphere and of the cyclotron mass with increasing pressure is observed on going to the GS. The minimal value of the cyclotron mass registered in the experiment was $\sim 1 \times 10^{-3} m_0$. A strong increase of the electron mobilities (up to $\sim 10^7 \text{ cm}^2/\text{V sec}$) was observed with decreasing gap ϵ_g . The main parameters of the registered spectrum of the alloys are determined for helium temperatures and at $p = 1 \text{ atm}$. In the low-temperature region, the semimetallic alloys $\text{Hg}_{1-x}\text{Cd}_x\text{Te}$ of p type exhibit an effect predicted by Gel'mont and D'yakonov,^[5] namely a decrease of the electron density with increasing temperature.

INTRODUCTION

1. Much interest has been shown recently in materials having a zero or anomalously small energy gap ϵ_g between the top of the valence band and the bottom of the conduction band. The peculiarities of the state of matter with $\epsilon_g = 0$, called the gapless state, was investigated theoretically in a number of studies^[1-6]. Much attention was paid to screening effects^[3-6], to the problem of hot carriers^[4], to impurity effects^[5], etc. In the case of band interaction, the smallness of ϵ_g leads to a strong nonparabolicity of the energy spectrum of the carriers^[7,8]. The character of the carrier dispersion laws in the gapless state was investigated in greatest detail in^[1-3].

2. Unique possibilities for the experimental study of the gapless state are afforded by alloys whose initial components have mutually inverted band spectra ($\text{Bi}_{1-x}\text{Sb}_x$ ^[9], $\text{Hg}_{1-x}\text{Cd}_x\text{Te}$ ^[10], $\text{Pb}_{1-x}\text{Sn}_x\text{Te}$ ^[11], etc.). In such systems, the direct gap ϵ_g varies smoothly with concentration x , and at a certain value of x (which in the general case depends on the temperature T) ϵ_g becomes equal to zero, i.e., the gapless state is realized. In a wide range of concentrations x , the inversion of terms in the alloys $\text{Bi}_{1-x}\text{Sb}_x$, $\text{Hg}_{1-x}\text{Cd}_x\text{Te}$, and $\text{Pb}_{1-x}\text{Sn}_x\text{Te}$, which leads to the transition to the gapless state, occurs under the influence of the pressure p ^[9,11-16], and in the alloys $\text{Bi}_{1-x}\text{Sb}_x$ the analogous transition is observed in the magnetic field H (the latter is connected with the fact that at certain orientations of H the spin splitting turns out to be larger than the orbital splitting)^[17]. Experimental investigations have shown that the transition to the gapless state is usually accompanied by a sharp decrease in the effective masses of the carriers (in the case of a linear dispersion law at $\epsilon_g = 0$ we have for the effective masses at the bottom of the band $m_i^*(0) = 0$) and by a strong increase in the mobilities^[9]. It should be noted that the distinguishing features of the transition to the gapless state become manifest most strongly at temperatures close to absolute zero, and at minimal concentrations of the impurity carriers.

3. One of the most convenient objects for the investigation of the transition to the gapless state at a pressure p are the alloys $\text{Hg}_{1-x}\text{Cd}_x\text{Te}$, which form a continuous series of solid solutions^[10]. These alloys have a zinc-

blende structure (the reduced Brillouin zone is a truncated octahedron). With increasing x , the energy spectrum of the alloys becomes smoothly restructured from the HgTe spectrum to the CdTe spectrum^[18].

The compound CdTe is a semiconductor with a direct gap $\epsilon_g = |\epsilon_{\Gamma_6} - \epsilon_{\Gamma_8}| \approx 1.6 \text{ eV}$ as $T \rightarrow 0^\circ\text{K}$. The semimetallic properties of HgTe are the result of inversion of the terms Γ_6 and Γ_8 . In the latter case the bottom of the conduction band is determined by the "light" branch Γ_8 , and the top of the valence band by the "heavy" branch Γ_6 ; the term Γ_6 (extremum with "light" holes) is under the term Γ_8 , at a depth $\sim 0.3 \text{ eV}$ at $T \approx 0^\circ\text{K}$. To avoid misunderstanding, we indicate that in this paper we take the gapless state of the alloys $\text{Hg}_{1-x}\text{Cd}_x\text{Te}$ to mean a state with $\epsilon_g = |\epsilon_{\Gamma_6} - \epsilon_{\Gamma_8}| = 0$. At the present time, there are several empirical relations, which are in qualitative agreement with one another^[19-21], for description of the dependence of the gap ϵ_g in the alloys $\text{Hg}_{1-x}\text{Cd}_x\text{Te}$ on the concentration x and on the temperature T . At helium temperatures, $\epsilon_g = 0$ at $x \approx 0.16$.

The absence of a symmetry center in the zincblende lattice leads to a certain shift of the maximum of the "heavy"-hole band away from the point $\mathbf{k} = 0$ ^[18], and as a result the valence band overlaps the conduction band (semimetallic phase) in HgTe and in $\text{Hg}_{1-x}\text{Cd}_x\text{Te}$ alloys with inverted band structure. The overlap ϵ_{OV} , incidentally, is small and does not exceed 10^{-3} eV ^[22].

The dispersion of the "light" electrons and "light" holes in HgTe and the $\text{Hg}_{1-x}\text{Cd}_x\text{Te}$ alloys is described quite adequately by the Kane model^[7]. The effective masses of the "light" carriers and the g -factor are then strongly dependent on ϵ_g . In the case of the transition to the gapless state, the carrier dispersion becomes linear, the masses at the bottom of the band vanish, and the spin splitting at the bottom of the band is equal to the orbital splitting^[23]. The parameters of the "heavy" holes are independent of ϵ_g in first-order approximation. At $T = 4.2^\circ\text{K}$ the electron effective mass in HgTe at the bottom of the band is $\sim 0.03 m_0$ ^[24], and the mass of the "heavy" holes is $\sim 0.4 m_0$ ^[25].

4. According to numerous data^[12-16], hydrostatic compression leads to a linear change in the quantity

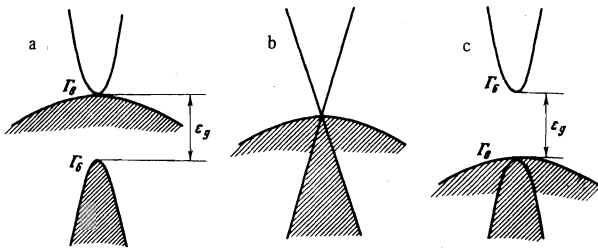


FIG. 1. Restructuring of the spectrum of semimetallic $\text{Hg}_{1-x}\text{Cd}_x\text{Te}$ alloys under pressure: a—spectra of the HgTe type at $p = 1$ atm; b—gapless state ($\epsilon\Gamma_6 - \epsilon\Gamma_8 = 0$) at $p = p_{c1}$; c—spectrum CdTe type (semiconducting phase) at $p > p_{c1}$.

$\epsilon_g = |\epsilon_{\Gamma_6} - \epsilon_{\Gamma_8}|$ at a rate $|\partial\epsilon_g/\partial p| = (10 \pm 2) \cdot 10^{-6}$ eV/atm for HgTe and $\text{Hg}_{1-x}\text{Cd}_x\text{Te}$ alloys in the semimetallic phase (Fig. 1). At a certain critical pressure p_c that depends on x and T ^[15], the alloys go over into the gapless state (Fig. 1b). Pressures $p > p_c$ transform the alloys into the semiconducting phase (Fig. 1c). No clear-cut dependence of $\partial\epsilon_g/\partial p$ on x or T has been observed in the region $0 \leq x < 0.2$.

5. In the case of a classical semiconductor whose direct gap ϵ_g separates "mirror" extrema with the Kane dispersion law, the impurity effects should depend to a strong degree on ϵ_g . Indeed, if the hydrogen model is correct, then the impurity-center ionization energy is $\epsilon_i \sim m^*(0)/\kappa^2$, and the Bohr radius is $a_B \sim \kappa/m^*(0)$ ($m^*(0)$ is the mass at the bottom of the band and κ is the dielectric constant). As $\epsilon_g \rightarrow 0$ we have $m^*(0) \rightarrow 0$, so that $\epsilon_i \rightarrow 0$ and a_B increases strongly. It is therefore clear that near the gapless state the impurity centers are ionized down to the lowest temperatures, the impurity carriers are in the corresponding bands, and the impurity-induced distortions of the carrier dispersion law are strongly decreased.

In the case of semimetallic $\text{Hg}_{1-x}\text{Cd}_x\text{Te}$ alloys, the situation is made more complicated by the presence of a band of "heavy" holes. In p-type alloys, the acceptor level, which is separated from the top of the valence band, falls into the region of allowed states of the conduction band^[12] and becomes quasilocal^[5] (the donor level, correspondingly, falls into the region of allowed states of the valence band). A detailed investigation of the peculiarities of the quasilocal impurity levels of HgTe, carried out in^[5], has shown that ϵ_i of the quasilocal acceptor levels becomes lower than ϵ_i of the local levels by an approximate factor of 2, and the levels themselves become smeared out, their half-widths being proportional to $(m_n/m_p)^{3/2}$, where m_n and m_p are respectively the electron and hole masses. It should be noted that the quasilocal character of the acceptor level should influence the critical concentration N_a of the acceptor centers, at which the levels become smeared out into an impurity band ($N_a a_B^3 \sim 1$). As shown in^[5], the wave function of a hole on a quasilocal acceptor level is more strongly "smeared out" in space than in the case of a local level. In view of this circumstance we can conclude that the impurity hole band in HgTe should appear already at $N_a \sim 10^{17}$ cm⁻³.

The calculations of^[5] have shown that the broadening of the donor levels in HgTe greatly exceeds their ionization energy, so that in general there is no localization of the impurity electrons on the donor centers.

6. A determination of the Hall mobility of n-type

semimetallic $\text{Hg}_{1-x}\text{Cd}_x\text{Te}$ alloys at helium temperatures has shown that μ_H is maximal for alloys with $\epsilon_g \rightarrow 0$ ^[13, 26]. In^[26], a theoretical analysis was carried out of the dependences of μ_H on x , using the assumption that the dominant scattering mechanism as $T \rightarrow 0^\circ\text{K}$ is scattering by an ionized impurity, and that the dielectric constant κ decreases linearly with increasing x , from $\kappa = 20$ for HgTe to $\kappa = 10.6$ for CdTe. In^[27, 28] they took account of the fact that the gap dependence of κ should have a singularity (minimum) near $\epsilon_g = 0$. It should be noted, however, that there is still no direct experimental proof of the existence of such a minimum for $\text{Hg}_{1-x}\text{Cd}_x\text{Te}$ alloys, probably owing to the insufficient purity and perfection of the available single crystals.

7. In the present investigation, we studied the singularities of pressure-induced transitions of $\text{Hg}_{1-x}\text{Cd}_x\text{Te}$ alloys of p-type with $0.1 < x < 0.15$ into the gapless state at pressures up to 15 katm and at temperatures $2^\circ\text{K} \leq T \leq 300^\circ\text{K}$. The investigations had a complex character: we studied both oscillatory effects (the Shubnikov-de Haas effect) and galvanomagnetic effects in weak magnetic fields ($\omega\tau \ll 1$). We have therefore obtained diverse data characterizing the energy spectrum of the investigated alloys in the semimetallic and semiconducting phases.

MEASUREMENT PROCEDURE, SAMPLES

Pressures up to 15 katm were produced by the method described in^[29]. The pressure-transmitting media were pentane-kerosene-oil mixtures. The galvanomagnetic coefficients in weak magnetic fields were measured by a null method. The accuracy of the electric measurements was 5×10^{-9} V. The temperature dependences of the resistivity ρ , of the Hall coefficient R_H and of the transverse-magnetoresistance coefficient $\Delta\rho/\rho H^2$ were measured in a cryostat with an automatic temperature regulator^[30].

The Shubnikov-de Haas effect was measured with an installation in which the $\rho(H)$ or $\partial\rho(H)/\partial H$ curves could be plotted automatically in magnetic fields up to 12 kOe. The measurements were performed with single-crystal nonoriented rectangular samples with typical dimensions $0.8 \times 0.8 \times 3$ mm. The current and potential leads (of 40 μ diameter) were soldered to the samples with indium solder. The composition of the investigated alloys was determined with a "CAMECA" microprobe x-ray analyzer.

MEASUREMENT RESULTS

1. Shubnikov-de Haas oscillations from the electron Fermi surface were observed at atmospheric pressure in all the investigated samples in the field interval $0 < H < 6$ kOe. When plotting the oscillation curves, particular attention was paid to elimination of superheat effects, which turned out to be appreciable even at currents of a few milliamperes flowing through the samples. The measurements were usually performed at currents less than 1 mA. With the exception of the region of magnetic fields near the quantum limit, the dependence of the number of oscillations on the reciprocal field was linear, making it possible to determine the period of the oscillations in the reciprocal field $\Delta(1/H) = eh/cS_{\text{extr}}$ ^[31] (S_{extr} is the extremal intersection of the Fermi surface and a plane perpendicular to the magnetic-field direction) with accuracy 10–20%. The independence of the period $\Delta(1/H)$, within the limits of the measurement

Certain parameters of the energy spectrum of the p-type $\text{Hg}_{1-x}\text{Cd}_x\text{Te}$ alloys investigated in the present paper at helium temperatures and $p = 1$ atm

Alloy	Number of sample	ϵ_g , meV	$N \cdot 10^{-15}$, cm^{-3}	$\frac{m_c(\epsilon_F)}{m_0} \cdot 10^3$	ϵ_F , meV	$\mu \cdot 10^{-4}$, $\text{cm}^2 \text{V}^{-1} \text{sec}^{-1}$	$P \cdot 10^{-17}$, cm^{-3}	$\nu \cdot 10^{-2}$, $\text{cm}^2 \text{V}^{-1} \text{sec}^{-1}$
$\text{Hg}_{0.98}\text{Cd}_{0.11}\text{Te}$	1-1	87	4.0	4.18	3.3	2.4	12	1.7
$\text{Hg}_{0.88}\text{Cd}_{0.12}\text{Te}$	1-2	69	0.57	0.69	3.8	4.5	6	2.0
$\text{Hg}_{0.87}\text{Cd}_{0.13}\text{Te}$	2-1	50	0.41	0.7	3.0	7.0	~ 1	—
$\text{Hg}_{0.9}\text{Cd}_{0.1}\text{Te}$	2-2	100	0.8	1.02	3.1	8.0	~ 1	—

error, of the orientation of the magnetic field is evidence of the sphericity of the electron Fermi surface. The cyclotron masses $m_c(\epsilon_F)$ at the Fermi level were determined from the temperature dependences of the $\rho(H)$ oscillation amplitude^[32] accurate to 20%. Detailed investigations of the influence of pressure on the Shubnikov oscillations, carried out for samples 2-1 and 2-2 (see the table), have shown that the oscillation period $\Delta(1/H)$ increases strongly with the pressure p , and that the region of existence of oscillations shifts systematically with increasing p towards weaker magnetic fields (Fig. 2). The oscillations vanish at pressures above a certain $p = p_{c1}$, which depends on the alloy composition (see the table).

Calculation has shown that the sections S_{extr} of the electron Fermi surface and the corresponding cyclotron masses $m_c(\epsilon_F)$ in the investigated alloys decrease linearly with increasing p (Fig. 3), the minimum value of $m_c(\epsilon_F)$, which was registered for the sample 2-1, amounting to $\sim 1 \times 10^{-3} m_0$.

The electron concentration N was determined from the relation

$$N[\text{cm}^{-3}] = \frac{p_F^3}{3\pi^2 \hbar^3} = \left(\frac{3.18 \cdot 10^6}{\Delta(1/H)[\text{Oe}^{-1}]} \right)^{3/2}$$

(p_F is the Fermi momentum), which is valid for a spherical Fermi surface.

Effects connected with the spin splitting of the Landau levels were not observed in this investigation.

2. In an investigation of galvanomagnetic effects in weak magnetic fields, we systematically monitored the width of the region of weak magnetic fields ($\omega\tau \ll 1$) at helium temperatures. It was established that the field H_c , the limit of the weak-field region, passes through a minimum with increasing pressure in all samples (Fig. 4). For sample 2-1, for example, at $T = 4.2^\circ\text{K}$ the region of weak magnetic fields narrows down to a few Oe at a pressure $p = p_{c1}$ corresponding to the minimum value of $m_c(\epsilon_F)$ for the electrons (Fig. 3). The decrease of H_c is obviously connected with the increase of the electron mobilities as $p \rightarrow p_{c1}$. Evidence favoring this assumption is provided by the very strong growth of the coefficient of transverse magnetoresistance $\Delta\rho/\rho H^2$ as $p \rightarrow p_{c1}$ for the investigated alloys at helium temperatures (Fig. 5). The Hall coefficient R_H , which is negative for all the investigated alloys at $p = 1$ atm and at helium temperatures, first increases noticeably in magnitude, reaches a maximum at $p \approx p_{c1}$, and then decreases abruptly and becomes positive at the highest pressures (Fig. 6). The inversion of the Hall coefficient R_H is accompanied by a decrease of $\Delta\rho/\rho H^2$ to a value $\sim 10^{-7} - 10^{-8} \text{Oe}^{-2}$.

For all the investigated alloys, the weakest dependence on the pressure was observed for the resistivity ρ (Fig. 7). In samples 1-1 and 1-2, which apparently



FIG. 2

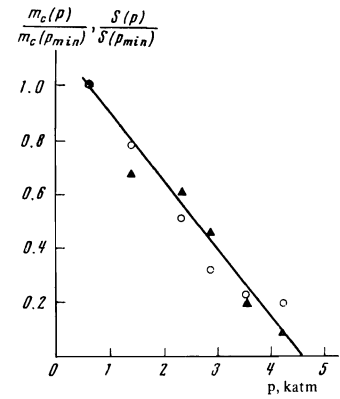


FIG. 3

FIG. 2. Field dependence of $\partial\rho/\partial H$ in sample 2-1 at $T = 2^\circ\text{K}$ and at different pressures $p < p_{c1}$: 1) $p = 36$ katm; 2) $p = 2.85$ katm; 3) $p = 3.5$ katm.

FIG. 3. Relative pressure dependence of the section S of the electron Fermi sphere (○) and of the cyclotron mass m_c at the Fermi level (▲) for sample 2-1 on going to the gapless state at helium temperatures.

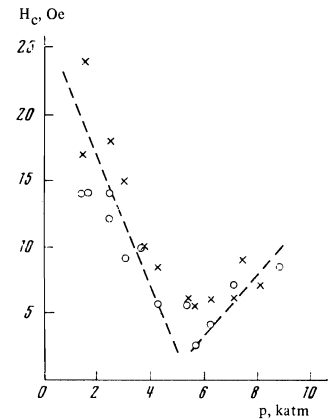


FIG. 4. Dependence of the magnetic field H_c that bounds the region of weak magnetic fields ($\omega\tau \ll 1$) on the pressure at $T = 4.2^\circ\text{K}$ for sample 2-1: X—determined from the field dependence of the Hall emf, ○—determined from the field dependence of the transverse-magnetoresistance coefficient.

have the maximum acceptor-defect concentration ($|R_H|$ is minimal after inversion), the resistivity ρ changes very little in the entire range of pressures p .

3. The temperature dependences of ρ , R_H , and $\Delta\rho/\rho H^2$ of the $\text{Hg}_{1-x}\text{Cd}_x\text{Te}$ alloys were plotted in the entire pressure interval. For samples 2-1 and 2-2, at pressures $p > p_{c1}$, sections with "semiconductor" behavior were observed on the plots of ρ against T ; these sections shifted towards higher temperatures with increasing pressure (Fig. 8). An estimate of the growth rate of the gap ϵ_g with pressure, based on these sections, yielded a value $\partial\epsilon_g/\partial p = (12 \pm 3) \times 10^{-6} \text{eV/atm}$, which agrees well with the data by others^[12-16]. It also follows from our dependences of ϵ_g on p that the gap $\epsilon_g \approx 0$ at $p = p_{c1}$ and as $T \rightarrow 0^\circ\text{K}$.

Low-temperature anomalies have been observed on the plots of $R_H(T)$ and $\Delta\rho/\rho H^2(T)$ at pressures somewhat lower than p_{c1} (Figs. 9, 10); these anomalies are particularly strong for samples 1-1 and 1-2. After inversion of R_H as a function of the pressure (at $p > p_{c2}$), the

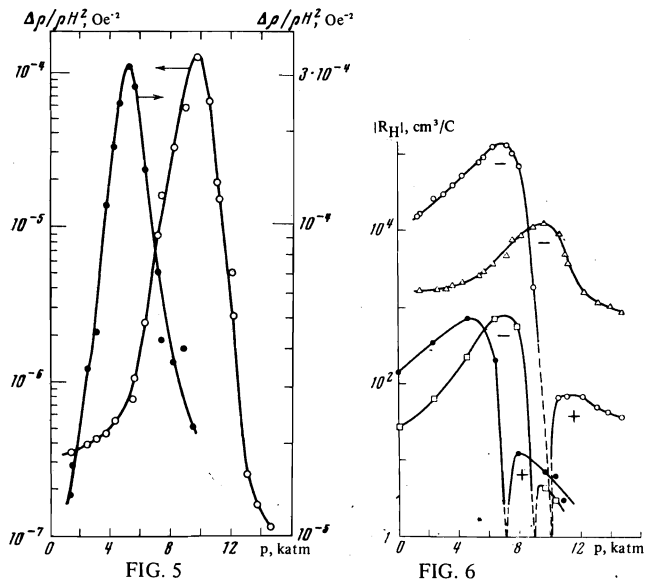


FIG. 5. Pressure dependence of the transverse magnetoresistance coefficient $\Delta\rho/\rho H^2$ at $T = 2^\circ\text{K}$ for samples 2-1 (\bullet , righthand scale) and 2-2 (\circ , lefthand scale).

FIG. 6. Pressure dependence of the modulus of the Hall coefficient $|R_H|$ at $T = 2^\circ\text{K}$ for samples 1-1 (\square), 1-2 (\bullet), 2-1 (\circ), and 2-2 (\triangle). The sign of the Hall coefficient is marked on the curves.

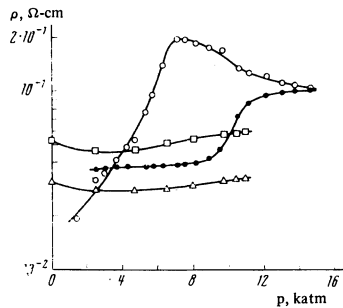


FIG. 7. Pressure dependence of the resistivity ρ at $T = 2^\circ\text{K}$ for the samples 1-1 (\triangle), 1-2 (\square), 2-1 (\circ), and 2-2 (\bullet).

temperature plots $R_H(T)$ of all the samples assumed the form typical of a semiconductor with an impurity hole band (Fig. 11).

DISCUSSION OF RESULTS

1. Singularities of the Transition of $\text{Hg}_{1-x}\text{Cd}_x\text{Te}$ Alloys into the Gapless State Under Pressure

As indicated in the Introduction, in the case of $\text{He}_{1-x}\text{Cd}_x\text{Te}$ alloys with $x < 0.16$ at helium temperatures, the inverted spectrum of the HgTe type is transformed under pressure into a spectrum of the CdTe type. Such a restructuring of the spectrum can be classified as a semimetal-semiconductor transition induced by pressure. During the course of this transition, the material is in the gapless state ($\epsilon_{\Gamma_6} - \epsilon_{\Gamma_8} \approx 0$) in a narrow interval of pressures near $p = p_{c1}$.

In the gapless state, the effective masses of the carriers are minimal, and the mobilities are maximal. Accordingly, the width of the region of weak magnetic fields ($\omega\tau \ll 1$) turns out to be smallest at $p = p_{c1}$ (Fig. 4), and the transverse magnetoresistance coefficient $\Delta\rho/\rho H^2$ reaches a maximum on going to the gapless state (Fig. 5). In this study, we have determined the pressure $p = p_{c1}$ of the transition to the gapless state

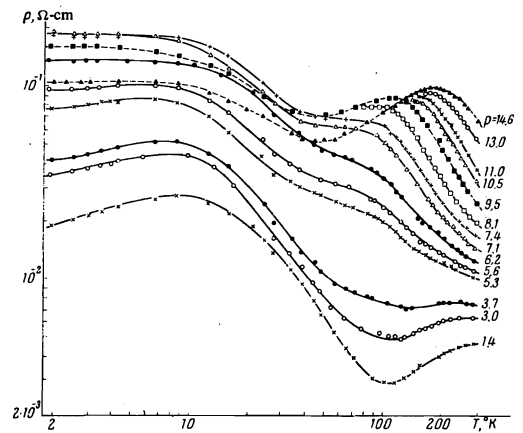


FIG. 8. Temperature dependences of the resistivity ρ at different pressures (in katm) for sample 2-1 (the values of the pressure correspond to the temperature $T = 4.2^\circ\text{K}$; the same holds for figures 9-11).

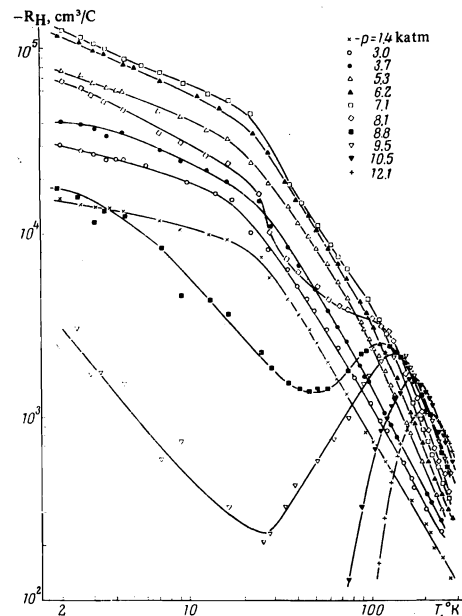


FIG. 9. Temperature dependences of the Hall coefficient at pressures $p < p_{c2}$ for sample 2-1.

both from the pressure dependences of $\Delta\rho/\rho H^2$ at helium temperatures and from the linear relations $\epsilon_g(p)$ obtained for the investigated alloys after their transition into the semiconducting phase (in the latter case, ϵ_g was determined from $\rho(T)$ in the high-temperature region (Fig. 8)). The values of p_{c1} determined by the two indicated methods were in good agreement; the error in the determination of p_{c1} did not exceed ± 0.5 katm.

It is obvious that after $\text{Hg}_{1-x}\text{Cd}_x\text{Te}$ goes over into the semiconducting phase under pressure the electric properties of the alloy at the lowest temperatures are determined exclusively by the nature of its defects. At a sufficiently large gap ϵ_g , the donor or acceptor levels in the semiconducting phase are in the region of forbidden energies, and a strong difference between the carrier masses at the bottom of the conduction band and at the top of the valence band should lead to a difference in the behavior of the n- and p-type alloys in the low-temperature region.

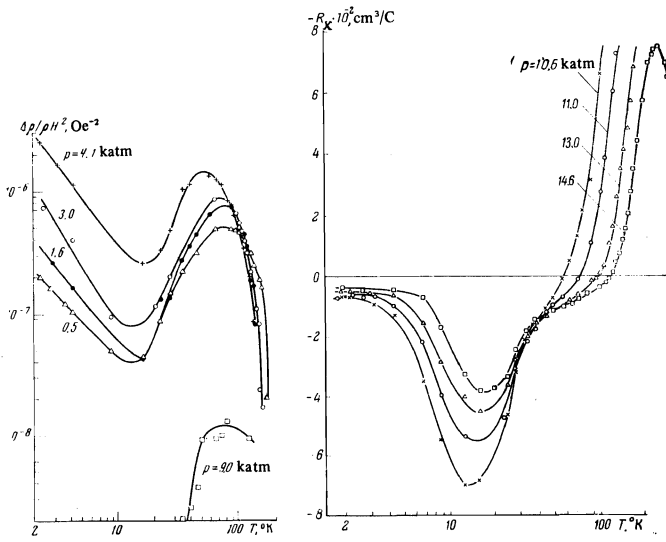


FIG. 10

FIG. 11

FIG. 10. Temperature dependence of the transverse magnetoresistance for sample 1-2 at different pressures.

FIG. 11. Temperature dependences of the Hall coefficient of sample 2-1 at pressures $p > p_{c1}$ (semiconducting phase).

In the case of the $\text{Hg}_{1-x}\text{Cd}_x\text{Te}$ alloys investigated by us at high pressures and in the semiconducting phase, the temperature dependences $\rho(T)$, $R_H(T)$ and $\Delta\rho/\rho H^2(T)$ acquire a form typical of a p-type semiconductor in which the conductivity as $T \rightarrow 0$ is determined by the conductivity in the hole impurity band (Figs. 8-11). With increasing temperature, the holes go over from the impurity band to the valence band, where their mobility is much higher. The resistivity ρ then decreases in a certain temperature interval $T < 70^\circ\text{K}$ (Fig. 8), and the hole Hall coefficient R_H goes through a characteristic maximum with increasing T (Fig. 11).

The character of the transition of the $\text{Hg}_{1-x}\text{Cd}_x\text{Te}$ into the gapless state should depend qualitatively on the type of defects (n- or p-type).

Let us consider the case of transition of a semimetallic $\text{Hg}_{1-x}\text{Cd}_x\text{Te}$ alloy of the p-type with large acceptor-defect concentration into the gapless state. In this material, a hole impurity band with large density of states is detached from the top of the valence band, and as $T \rightarrow 0^\circ\text{K}$ the Fermi level ϵ_F is situated in this band. The overlap of the hole impurity band with the conduction band causes the electrons to fill the conduction band up to $\epsilon = \epsilon_F$ (Fig. 12). The parameters of the valence band Γ_8 with "heavy" holes, from which the impurity band is detached, do not depend on ϵ_g . One can therefore expect the Fermi level to become frozen into the impurity band at $P \gg N$ and to be independent of p (i.e., of ϵ_g), so that the electron Fermi energy ϵ_F becomes fixed¹⁾.

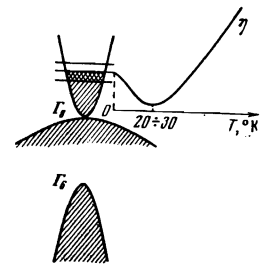
It is known that in the case of small values of ϵ_g , the Kane dispersion law takes the form

$$\epsilon \left(1 + \frac{\epsilon}{\epsilon_g} \right) = \frac{p^2}{2m^*(0)}, \quad (1)$$

$$m^*(0) = \frac{3}{4} \frac{\hbar^2 \epsilon_g}{\mathcal{P}^2} = \alpha \epsilon_g,$$

where $m^*(0)$ is the mass at the bottom of the band and \mathcal{P}

FIG. 12. Qualitative form of the energy spectrum of the semimetallic p-type $\text{Hg}_{1-x}\text{Cd}_x\text{Te}$ alloys investigated in the present study at $p < p_{c1}$. The figure shows the motion of the chemical potential η with increasing temperature in the low-temperature region.



is the matrix element of the momentum operator. The cyclotron mass $m_c(\epsilon_F)$ at the Fermi level is given by

$$m_c(\epsilon_F) = m^*(0) \left(1 + \frac{2\epsilon_F}{\epsilon_g} \right). \quad (2)$$

We denote the fixed value by $\epsilon_F \equiv \delta$. We then obtain for the section S of the Fermi sphere and for the cyclotron mass $m_c(\epsilon_F)$

$$S = 2\pi m^*(0) \epsilon_F \left(1 + \frac{\epsilon_F}{\epsilon_g} \right) = 2\pi \alpha \delta (\epsilon_g + \delta), \quad (3)$$

$$m_c(\epsilon_F) = \alpha (\epsilon_g + 2\delta). \quad (4)$$

It is seen from (3) and (4) that S and $m_c(\epsilon_F)$ are linear in ϵ_g in the case of a fixed Fermi energy.

For the electron concentration N raised to the $2/3$ ($N^{2/3} \sim S$) we have

$$N^{2/3} = (3\pi^2 \hbar^3)^{-2/3} [2\alpha \delta (\epsilon_g + \delta)]. \quad (5)$$

Thus, $N^{2/3}$ also varies linearly with the gap ϵ_g .

It follows from (3)-(5) that the experimentally determined gap dependences of S , m_c , and $N^{2/3}$ enable us to find the matrix element \mathcal{P} and the Fermi energy $\epsilon_F \equiv \delta$.

If the transition to the gapless state is produced in an n-type $\text{Hg}_{1-x}\text{Cd}_x\text{Te}$ alloy in which ϵ_F exceeds the overlap energy ϵ_{ov} , then the electron concentration N and, consequently, S do not depend on ϵ_g . We put $S \equiv Q$ for the fixed value. We then obtain for ϵ_F

$$\epsilon_F = -\frac{\epsilon_g}{2} + \left[\left(\frac{\epsilon_g}{2} \right)^2 + \frac{Q}{2\pi\alpha} \right]^{1/2}, \quad (6)$$

from which we see that ϵ_F reaches a maximum in the gapless state.

The cyclotron mass $m_c(\epsilon_F)$ depends on ϵ_g in a non-linear manner:

$$m_c(\epsilon_F) = 2\alpha \left[\left(\frac{\epsilon_g}{2} \right)^2 + \frac{Q}{2\pi\alpha} \right]^{1/2}. \quad (7)$$

We note that the last case is apparently realized when semiconducting $\text{Bi}_{1-x}\text{Sb}_x$ alloys go over into the gapless state under pressure^[9].

The helium-temperature gap ϵ_g of the $\text{Hg}_{1-x}\text{Cd}_x\text{Te}$ alloys investigated in the present study can be determined for any pressure, including atmospheric, from the formula

$$\epsilon_g = \left| \frac{\partial \epsilon_g}{\partial p} \right|_{p_{c1-p}}. \quad (8)$$

As already indicated, the most probable value is $|\partial \epsilon_g / \partial p| = (10 \pm 2) \cdot 10^{-6} \text{ eV/atm}^{[12, 16]}$.

A calculation of ϵ_F from the values of S , $m_c(\epsilon_F)$ and ϵ_g with the aid of relations (2), (3), and (8), carried out for samples 2-1 and 2-2, has shown that ϵ_F does not

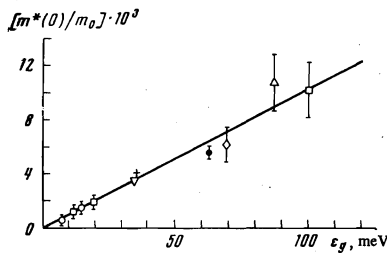


FIG. 13. Dependence of the electron effective mass at the bottom of the band $m^*(0)$ on the gap ϵ_g in $\text{Hg}_{1-x}\text{Cd}_x\text{Te}$ alloys: Δ —sample 1-1, \diamond —sample 1-2, \circ —sample 2-1, \square —sample 2-2, ∇ —from [33], $+,-$ from [21], \bullet —from [34].

vary noticeably with pressure. The constancy of ϵ_F , and also the linear decrease of the sections S and of the cyclotron masses $m_c(\epsilon_F)$ with p (i.e., with ϵ_g) (Fig. 3) favor the correctness of the model proposed in the present paper for description of the transition of semimetallic p-type $\text{Hg}_{1-x}\text{Cd}_x\text{Te}$ alloys into the gapless state.

The variation of the galvanomagnetic coefficients of the investigated alloys with pressure can be described qualitatively in the following manner.

At helium temperatures the semimetallic p-type $\text{Hg}_{1-x}\text{Cd}_x\text{Te}$ alloys with acceptor defect concentration $\geq 10^{17} \text{ cm}^{-3}$ have two groups of carriers: "light" electrons at the bottom of the conduction band and "heavy" holes in the hole impurity band. The electron concentration is determined by the position of the Fermi level ϵ_F , which is frozen into the impurity band, and by the gap ϵ_g , on which the density of states in the conduction band depends. An increase of the pressure decreases $|\epsilon_g|$, and consequently decreases the effective masses and the state density in the conduction band. The position of the Fermi level remains unchanged in this case, since the hole impurity band parameters do not depend significantly on ϵ_g . A decrease of the state density in the conduction band leads to a decrease in the electron concentration N in this band, in accordance with (5). The values of S and $m_c(\epsilon_F)$ vary in accord with (3) and (4). At the pressure $p = p_{c1}$ the gap $\epsilon_g \approx 0$; the mass at the bottom of the conduction band is in this case $m^*(0) \approx 0$.

The electron mobility μ reaches a maximum value when the alloys go over into the gapless state ($p = p_{c1}$). The transverse magnetoresistance coefficient $\Delta\rho/\rho H^2$, which depends strongly on the mobility, also reaches a maximum on going to the gapless state. The electronic contribution to R_H , in view of the fact that the electron mobilities μ are much higher than the hole mobilities ν , turns out to be predominant at all $p \leq p_{c1}$ and helium temperatures. The decrease of N in the conduction band with pressure leads to a growth of R_H . After the gapless state is eliminated ($p > p_{c1}$) the overlap of the conduction band (Γ_6) and of the hole impurity band decreases rapidly. The electron concentration N vanishes at a $p = p_{c2}$ given by the relation

$$\delta = \frac{\partial \epsilon_g}{\partial p} (p_{c2} - p_{c1}).$$

The Hall coefficient R_H is inverted in this case, and $\Delta\rho/\rho H^2$ decreases to values $10^{-7} = 10^{-8} \text{ Oe}^{-2}$ owing to the smallness of the hole mobilities ν in the impurity band.

2. Change of Carrier Effective Mass, Concentration, and Mobility on going to the Gapless State

The electron effective masses at the bottom of the

band $m^*(0)$ of the investigated alloys at various pressures were determined from $m_c(\epsilon_F)$, ϵ_F , and ϵ_g with the aid of relation (2). The dependence of $m^*(0)$ on the gap ϵ_g is shown in Fig. 13. The same figure shows the data of [21, 23, 34]. In accordance with the Kane model, the gap dependence of $m^*(0)$ is linear, and the matrix element \mathcal{P} turns out to equal $\sim 7.1 \times 10^{-8} \text{ eV}\cdot\text{cm}$. The available data allow us to conclude that for $\text{Hg}_{1-x}\text{Cd}_x\text{Te}$ alloys with $x < 0.2$ the value of \mathcal{P} does not depend significantly on x .

The electron concentration N , the electron mobility μ , and the product $P\nu$ of the hole concentration by the hole mobility were calculated from the given ρ , R_H , and $\Delta\rho/\rho H^2$ on the basis of the two-band model. The corresponding formulas in the case $N\mu^2 \gg P\nu^2$ (it is possible here that $P \gg N$ and $P\nu \sim N\mu$) can be represented in the form

$$1/\rho = \sigma = e(P\nu + N\mu), \quad (9)$$

$$R_H = -\frac{1}{e} \frac{N\mu^2}{(P\nu + N\mu)^2}, \quad (10)$$

$$\frac{\Delta\rho}{\rho H^2} = \frac{P\nu N\mu^3}{(P\nu + N\mu)^2}. \quad (11)$$

From an examination of the plots of ρ , R_H , and $\Delta\rho/\rho H^2$ against p (Figs. 5–7), from the point of view of relations (9)–(11), we can conclude the following. The hole contribution $eP\nu$ to the mobility should not vary strongly on going to the gapless state. The electron contribution eN to the mobility can vary in a complicated manner with pressure, inasmuch as the concentration N decreases on going to the gapless state, and the mobility μ increases (the electron contribution $eN\mu$ vanishes when the alloys go over into the semiconducting phase). It is clear that at $eP\nu > eN\mu$ the hole contribution stabilizes the $\rho(p)$ dependence (Fig. 7). Relations (10) and (11) remain in force in the region $p < p_{c1}$ even in the case $P\nu > N\mu$, if $\mu \gg \nu$.

On going to the gapless state, the strongest increase occurs in $\Delta\rho/\rho H^2$, inasmuch as (11) contains μ^3 (Fig. 5). It follows from the two-band model that R_H is inverted after the electrons vanish, and $\Delta\rho/\rho H^2 \rightarrow 0$ (it appears that the simplified relation (10) ceases to hold as soon as $p > p_{c1}$).

The formalism considered above is naturally only a certain approximation, but the strong variation of the galvanomagnetic coefficients (Figs. 5–7) on going from the two-band spectrum ($p < p_{c2}$) to the one-band spectrum ($p > p_{c2}$) allows us to assume that the two-band character of the spectrum fully determines the features of the transport phenomenon in our case.

Calculations have shown that the values of N determined from (9)–(11) and from the Shubnikov oscillations are in good agreement, thus confirming the correctness of the calculations.

Certain parameters obtained from the calculations and characterizing the $\text{Hg}_{1-x}\text{Cd}_x\text{Te}$ alloys at $p = 1 \text{ atm}$ and at helium temperatures are listed in the table.

As indicated above, the model assumed in the present paper for description of the transition of p-type $\text{Hg}_{1-x}\text{Cd}_x\text{Te}$ alloys into the gapless state predicts a linear gap dependence for $N^{2/3}$ on ϵ_g for four p-type $\text{Hg}_{1-x}\text{Cd}_x\text{Te}$ alloys investigated in the present paper are shown in Fig. 14. The solid lines in the figure were drawn in accordance with formula (5) for $\mathcal{P} = 7.1$

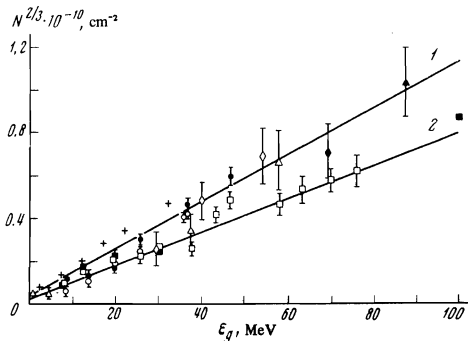


FIG. 14. Dependence of the electron concentration N raised to the $2/3$ power on the gap ϵ_g at $T = 2^\circ\text{K}$ for p-type $\text{Hg}_{1-x}\text{Cd}_x\text{Te}$ alloys: Δ, \blacktriangle —sample 1-1, \blacklozenge, \circ —1-2, \bullet, \circ —2-1, \square, \blacksquare —2-2. Dark point—from oscillation-measurement data, light points—calculated from galvanomagnetic effects in weak magnetic field. $+$ —sample 7B of [12]. The solid straight lines 1 and 2 were calculated from formula (5) at $\mathcal{P} = 7.1 \times 10^{-8}$ eV-cm and at $\delta = 3.5$ and 2.5 meV, respectively.

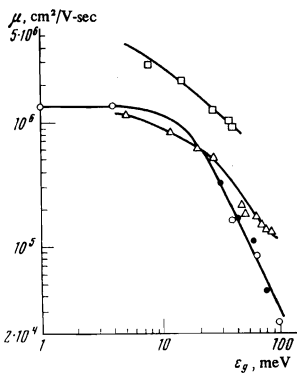


FIG. 15. Dependence of the electron mobility μ on the gap ϵ_g at $T = 2^\circ\text{K}$ in the investigated p-type $\text{Hg}_{1-x}\text{Cd}_x\text{Te}$ alloys: \circ —sample 1-1, \bullet —1-2, \circ —2-1, \triangle —2-2.

$\times 10^{-8}$ eV-cm and for δ equal to 2.5 and 3.5 MeV. As seen from Fig. 14, in first-order approximation a linear gap dependence of $N^{2/3}$ is observed for all alloys, and the electron Fermi energies $\epsilon_F \equiv \delta$ are very close in magnitude, in spite of the considerable difference between the concentrations of the acceptor defects (see the table).

Figure 14 also shows the dependence of $N^{2/3}$ on ϵ_g obtained for the p-type alloy $\text{Hg}_{1-x}\text{Cd}_x\text{Te}$ ($x = 0.149$) (Sample 7B) in [12]. It should be noted that the value $\epsilon_F = 3 \pm 0.5$ meV determined in the present paper for p-type $\text{Hg}_{1-x}\text{Cd}_x\text{Te}$ alloys agrees with the ionization energy $\epsilon_i \approx 6$ meV of a single quasilocal acceptor level, as calculated in [5] for HgTe, if account is taken of the fact that when the impurity band is produced its center of gravity shifts towards the boundary of the main band [35]. The reasons for observing much larger values of $\epsilon_F \equiv \delta$ (up to 20 meV) in [12] remain unclear.

Calculations have shown that the electron mobilities μ of the investigated alloys increase strongly with decreasing gap in a wide range of values of ϵ_g , in proportion to $\epsilon_g^{-\gamma}$ (where $1 \leq \gamma \leq 2.4$), approaching 10^7 cm²/V-sec in sample 2-1 at helium temperatures on going over to the gapless state (Fig. 15). These relations are in qualitative agreement with the results of [12]. The much weaker growth of the mobilities with decreasing gap ϵ_g that was observed in the semimetallic n-type $\text{Hg}_{1-x}\text{Cd}_x\text{Te}$ alloys at $T = 4.2^\circ\text{K}$ in [13] seems to be due to the fact that the samples were polycrystalline.

Expressions for the electron mobility μ of $\text{Hg}_{1-x}\text{Cd}_x\text{Te}$ alloys in the case of scattering by an

ionized impurity were obtained in a number of papers [26-28]. It is easy to verify that if ϵ_F is constant and the variation of the dielectric constant κ can be neglected, then the dependence of μ on ϵ_g takes the form $\mu \propto \epsilon_g^{-1/2}$ [26] at pressures $p < p_{c1}$ (when $\epsilon_F \ll \epsilon_g$).

Allowance for the anomaly of κ as $\epsilon_g \rightarrow 0$ [27, 28] can only weaken this dependence. The strong power-law dependence of μ on ϵ_g observed in the present study therefore cannot be explained on the basis of the indicated model. It is not excluded that an appreciable contribution to the carrier scattering at helium temperatures is made by interband scattering (conduction band-impurity band), but it is difficult at present to obtain quantitative estimates.

It should be noted that when n-type $\text{Hg}_{1-x}\text{Cd}_x\text{Te}$ alloys go over into the gapless state the $\mu(\epsilon_g)$ dependence at $T = 4.2^\circ\text{K}$ should be stronger than for p-type $\text{Hg}_{1-x}\text{Cd}_x\text{Te}$ alloys, inasmuch as in this case the electron Fermi energy ϵ_F reaches a maximum at $\epsilon_g = 0$ (see (6)).

Calculation shows that the quantity $P\nu$, which characterizes the hole contribution to the conductivity, decreases monotonically with pressure as $p \rightarrow p_{c1}$; the change in $P\nu$ does not exceed 30% in this case.

The hole contribution to the conductivity at helium temperatures and at $p = 1$ atm turned out to be quite appreciable in the investigated alloys. Thus, in samples 1-1 and 1-2, with respective hole densities $\sim 12 \times 10^{17}$ and $\sim 6 \times 10^{17}$ cm⁻³, the conductivity for the hole impurity band was $\geq 80\%$ of the total conductivity (see the table). The hole density and the hole mobility were estimated from ρ and R_H at $p > p_{c2}$, when the alloys went over into the semiconducting phase. The appreciable value of the hole mobility (see the table) in the impurity band appears to be connected with the characteristic broadening of the wave functions of the states at the impurity levels [5].

Tentative calculations of the pressure dependences of μ and N in the investigated alloys at $T > 4.2^\circ\text{K}$ (Figs. 16 and 17) have shown that, as expected, the maxima on the $\mu(p)$ curves shift towards lower pressures with increasing T ($|\epsilon_g|$ decreases with increasing T). However, the shift of the maximum in the low-temperature interval is weaker than would follow from the dependence of ϵ_g on x and T [19-21]. The reasons for this discrepancy are not clear.

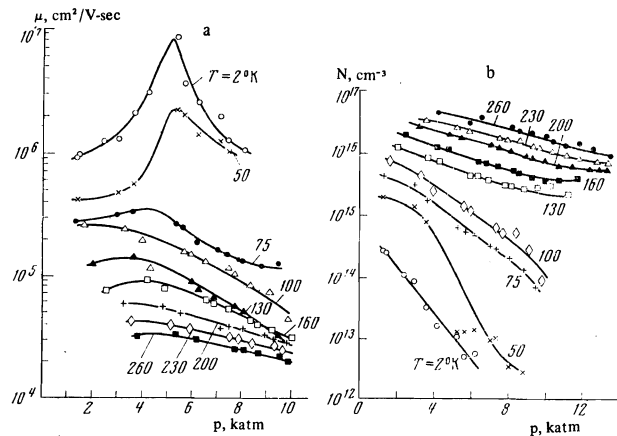


FIG. 16. Plots of the electron mobility (a) and of the electron density (b) against the pressure at various temperatures for sample 2-1.

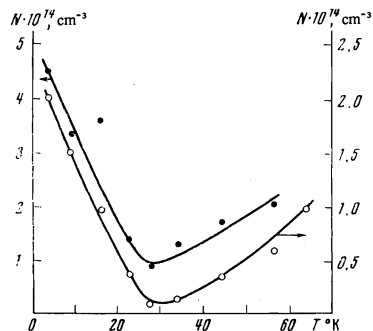


FIG. 17. Temperature dependence of the electron density N at $p = 4.4$ $\text{katm} < p_{C1}$ for samples 1-1 (\bullet , left-hand scale) and 1-2 (\circ , right-hand scale).

3. Low-Temperature Anomalies of $R_H(T)$ and $\Delta\rho/\rho H^2(T)$

Low-temperature anomalies on the $R_H(T)$ curves, analogous to those shown in Fig. 9, were observed in p-type $\text{Hg}_{1-x}\text{Cd}_x\text{Te}$ alloys by a number of workers^[36,37]. In the present study we observed anomalies of similar type also in the plots of $\Delta\rho/\rho H^2$ against T (Fig. 10).

It is indicated in^[5] that such anomalies in p-type HgTe may be due to the decrease of the electron density N with increasing T in the low-temperature region. According to the calculations in^[5], the dependence of N on T has a minimum at $kT \sim \epsilon_i/2$, where ϵ_i is the ionization energy of the quasiloocal acceptor level.

The effect predicted in^[5] is due to the specific character of the temperature dependence of the chemical potential in doped semiconductors. As is well known, the chemical potential of a standard semiconductor with a hole impurity band lies in the impurity band at $T = 0^\circ\text{K}$. With increasing T it first shifts toward the top of the valence band, and only then does it move to the center of the gap ϵ_g . In the cases of HgTe and of $\text{Hg}_{1-x}\text{Cd}_x\text{Te}$ alloys with sufficient acceptor-defect concentration, a similar motion of the chemical potential should be observed with increasing T (Fig. 12). The electron density N would then decrease in the temperature region where the chemical potential drops.

A calculation carried out in the present study for samples 1-1 and 1-2 with the maximum acceptor-defect concentration have shown that the effect predicted in^[5] does indeed take place (Fig. 17). The decrease of N in the low-temperature interval with increasing T is accompanied by a strong decrease of the electron mobility μ and by an increase of $P\nu$.

The calculation results suggest the following model for explanation of the low-temperature anomalies on the $R_H(T)$ and $\Delta\rho/\rho H^2(T)$ curves of p-type $\text{Hg}_{1-x}\text{Cd}_x\text{Te}$ alloys. The intense transitions of the holes from the impurity band to the valence band, which occur in the low-temperature interval (the process is clearly seen in Fig. 11) lead to a lowering of the chemical potential. This process is accompanied by a decrease of the electron density N and mobility μ , which in the case of scattering by an ionized impurity is very sensitive to ϵ_F ($\mu \sim \epsilon_F^{3/2}$). At the same time, owing to the transitions of the holes into the valence band, the average hole mobility increases. As a result, the electron contribution to the galvanomagnetic coefficients decreases, and the hole

contribution increases. After the transfer of the holes from the impurity band to the valence band is completed, the chemical potential begins to rise rapidly with increasing temperature, and this leads to an increase in the electron density N with temperature. The thermal generation of fast electrons causes an increase of R_H and $\Delta\rho/\rho H^2$ in a certain temperature interval. With further growth of T , the material goes over into the intrinsic-conductivity state.

In conclusion, we take the opportunity to express sincere gratitude to S. D. Beneslavskii, V. L. Bonch-Bruевич, and B. L. Gel'mont for exceedingly useful discussions. The authors are grateful to V. I. Ivanov-Omskii and V. K. Ogorodnikov for a number of valuable remarks.

- ¹ A. A. Abrikosov and S. D. Beneslavskii, *Zh. Eksp. Teor. Fiz.* **59**, 1280 (1970) [*Sov. Phys.-JETP* **32**, 699 (1971)].
- ² A. A. Abrikosov and S. D. Beneslavskii, *J. Low Temp. Phys.* **5**, 141, 1971.
- ³ A. A. Abrikosov, *J. Low Temp. Phys.* **8**, 315, 1972.
- ⁴ S. D. Beneslavskii, *Fiz. Tverd. Tela* **13**, 1727 (1971) [*Sov. Phys.-Solid State* **13**, 1444 (1971)].
- ⁵ B. L. Gel'mont and M. I. D'yakonov, *Zh. Eksp. Teor. Fiz.* **62**, 713 (1972) [*Sov. Phys.-JETP* **35**, 377 (1972)].
- ⁶ L. Liu and D. Brust, *Phys. Rev.* **173**, 777, 1968.
- ⁷ E. O. Kane, *J. Phys. Chem. Sol.* **1**, 249, 1957.
- ⁸ M. H. Cohen, *Phys. Rev.* **121**, 387, 1961.
- ⁹ N. B. Brandt, Ya. G. Ponomarev, and S. M. Chudinov, *J. Low Temp. Phys.* **8**, 369, 1972.
- ¹⁰ D. Long and J. L. Schmit, *Semiconductors and Semimetals*, **5**, ed. by R. K. Willardson and A. C. Beer, Academic, New York, 1970, p. 175.
- ¹¹ In: *Poluprovodniki s uzkoj zapreshchenoi zonoj i ikh primeneniye* (Semiconductors with Narrow Forbidden Bands and their Applications), Russ. Transl., Mir, 1969.
- ¹² C. T. Elliott, J. Melngailis, T. C. Harman, J. A. Kafalas, and W. C. Kernan, *Phys. Rev.* **B5**, 2985, 1972.
- ¹³ J. Stankiewicz, W. Giriat and A. Bienenstock, *Phys. Rev.* **B4**, 4465, 1971.
- ¹⁴ G. Weill and C. Vérié, *C. R. Acad. Sci., Paris*, **263**, 463, 1966.
- ¹⁵ J. Stankiewicz and W. Giriat, *Phys. Stat. Sol. (b)*, **49**, 387, 1972.
- ¹⁶ M. I. Daunov and E. L. Broyda, *Phys. Stat. Sol. (b)*, **55**, K155, 1973.
- ¹⁷ N. B. Brandt and E. A. Svistova, *J. Low Temp. Phys.* **2**, 1, 1970.
- ¹⁸ Shin-ichi Katsuki, and M. Kunimune, *J. Phys. Soc. Japan* **31**, 415, 1971.
- ¹⁹ M. W. Scott, *J. Appl. Phys.* **40**, 4077, 1969.
- ²⁰ J. L. Schmit and E. L. Stelzer, *J. Appl. Phys.* **40**, 4865, 1969.
- ²¹ J. D. Wiley and R. N. Dexter, *Phys. Rev.* **181**, 1181, 1969.
- ²² V. V. Sologub, V. I. Ivanov-Omskii, V. M. Muzhdaba, and S. S. Shalyt, *Fiz. Tekh. Poluprov.* **4**, 1736 (1971) [*Sov. Phys.-Semicond.* **4**, 1489 (1971)].
- ²³ W. Zawadzki, *Phys. Lett.* **4**, 190, 1963.
- ²⁴ R. Stradling, *Proc. Phys. Soc.* **90**, 175, 1967.
- ²⁵ R. Stradling and G. Antcliffe, *Proc. Intern. Confer. Semicond. Physics, Kyoto*, 1966, p. 374.
- ²⁶ D. Long, *Phys. Rev.* **176**, 923, 1968.

- ²⁷ V. I. Ivanov-Omskiĭ, B. T. Kolomiets, V. K. Ogorodnikov, and K. P. Smekalova, *Fiz. Tekh. Poluprov.* **4**, 264 (1970) [*Sov. Phys.-Semicond.* **4**, 214 (1970)].
- ²⁸ B. G. Gel'mont, V. I. Ivanov-Omskiĭ, B. T. Kolomiets, V. K. Ogorodnikov, and K. P. Smekalova, *ibid.* **5**, 266 (1971) [**5**, 228 (1971)].
- ²⁹ N. B. Brandt and Ya. G. Ponomarev, *Zh. Eksp. Teor. Fiz.* **55**, 1215 (1968) [*Sov. Phys.-JETP* **28**, 635 (1969)].
- ³⁰ Ya. G. Ponomarev, *Prib. Tekh. Eksp.* **6**, 218 (1966).
- ³¹ I. M. Lifshitz and A. M. Kosevich, *Zh. Eksp. Teor. Fiz.* **29**, 329 (1955) [*Sov. Phys.-JETP* **2**, 187 (1956)].
- ³² E. Adams and T. Holstein, *J. Phys. Chem. Sol.* **10**, 254, 1959.
- ³³ T. Harman, *J. Phys. Chem. Sol.* **25**, 931, 1964.
- ³⁴ G. A. Antcliffe, *Phys. Rev.* **B2**, 345, 1970.
- ³⁵ V. L. Bonch-Bruevich, in: *Fizika tverdogo tela (Solid State Physics)*, VINITI, 1965.
- ³⁶ Osamu Ohtsuki, Ryuichi Veda, Koji Shinohara, and Yoichi Veda, *Japan J. Appl. Phys.* **10**, 1288, 1971.
- ³⁷ V. V. Patashinskiĭ and P. S. Kireev, *Tezisy dokladov III simpoziuma po polymetallam i poluprovodnikam s maloĭ shirinoĭ zapreshchennoĭ zony (Abstracts of Papers, Third Symposium on Semimetals and Semiconductors with Narrow Forbidden Bands)*, L'vov, 1972, p. 13.

Translated by J. G. Adashko

34